UCRL-JRNL-210010

LAWRENCE
LIVERMORE
NATIONAL
LABORATORY

Characterization of the restricted rotation of the dimethyl groups in chemically N-terminal 13C labeled Antifreeze Glycoproteins: A temperature dependent study in water to ice through the supercooled state.

V. V. Krishnan, E. Y. Lau, N. M.Tsvetkova, R. E. Feeney, W. H. Fink, Y. Yeh

February 25, 2005

Journal of Chemical Physics

Disclaimer

This document was prepared as an account of work sponsored by an agency of the United States Government. Neither the United States Government nor the University of California nor any of their employees, makes any warranty, express or implied, or assumes any legal liability or responsibility for the accuracy, completeness, or usefulness of any information, apparatus, product, or process disclosed, or represents that its use would not infringe privately owned rights. Reference herein to any specific commercial product, process, or service by trade name, trademark, manufacturer, or otherwise, does not necessarily constitute or imply its endorsement, recommendation, or favoring by the United States Government or the University of California. The views and opinions of authors expressed herein do not necessarily state or reflect those of the United States Government or the University of California, and shall not be used for advertising or product endorsement purposes.

Characterization of the restricted rotation of the dimethyl groups in chemically N-terminal ^{13}C labeled Antifreeze Glycoproteins: A temperature dependent study in water to ice through the supercooled state.

V. V. Krishnan[1*], Edmond Y. Lau[1], Nelly M. Tsvetkova[2], Robert E. Feeney[3], William H. Fink[4] and Yin Yeh[5].

[1]Biosciences Directorate, Lawrence Livermore National Laboratory, Livermore, CA 94551, [2]Section of Molecular and Cellular Biology, [3]Department of Food Science and Technology, [4]Department of Chemistry and [5] Department of Applied Science, University of California, Davis, CA 95616

[*]Corresponding Author

krish@llnl.gov

(925) 422-3329 (phone), (925) 424-3130 (fax)

Abstract

Site-specific chemical modification, especially with isotopically enriched groups, allows one to study the structure and dynamics of proteins for which uniform enrichment is difficult. When the N-terminal alanine in antifreeze glycoprotein (AFGP), is replaced with an N,N-dimethyl alanine the methyl groups show signatures of slow rotation about the C-N bond. In order to separate the local dynamics of the N-terminus from the overall protein dynamics, we present a complete characterization of this dynamics. Temperature dependent NMR experiments from room temperature to sub-zero temperatures, including the supercooled state and in the presence of ice, are presented. Quantum chemical calculations are also performed on a localized N-terminus of the AFGP. Our results show that in the solution state at room temperature and in supercooled regime, the dimethyl groups undergo a slow, restricted rotation with an unequal distribution of population between two major conformations. At further lower temperatures in the presence of ice, the dynamics become much more complex due to freezing out of several conformational states. Based on these results, we conclude that the segmental dynamics of the N-terminus are local to the first residue and do not affect the overall dynamics of the protein.

Key Words

AFGP (Antifreeze Glycoproteins), Protein dynamics, NMR, Supercooled water, ice.

I Introduction

Chemical modification of protein backbone and side-chains is an important tool to investigate site-specific structural and dynamical information in proteins. The choices of which site to modify, and which chemical label to use, are driven by how well the site can be modified without compromising protein function. Chemical labeling by isotopic enrichment of radioactive atoms such as ^{32}P and ^{14}C have been used extensively to monitor enzyme activity and intermolecular interactions [1]. Nuclear magnetic resonance (NMR) spectroscopy has become a powerful tool to study protein structure and dynamics with atomic level details and an integral part of structural biology [2]. This progress is made possible due to advances in both high level production of uniformly enriched ($^{15}N/^{13}C$) proteins and the design of new experimental methods to effectively use such developments [3]. However, not all proteins can be expressed in external cells such as *E.Coli*, and it is particularly difficult for membrane proteins and glycoproteins [4]. Antifreeze glycoproteins (AFGP) are present only in certain fishes at Antarctica so that they can survive even at sub-zero temperatures [5-7]. Recently, we have used the chemical labeling of AFGP molecules, with ^{13}C enriched dimethyl group (N-terminal alanine replaced by N,N-dimethyl alanine) to investigate structure and dynamics in the presence of ice using solid-state NMR and FT-IR methods [8]. In this work we present a comprehensive characterization of the N-terminal dynamics using NMR spectroscopy and quantum chemical calculations. NMR experiments were performed in the solution state (room temperature) through the supercooled state (sub-zero temperatures to -17° C) including the solid-state (in the presence of ice to –80 °C). As dynamics of the chemical label also reflect the dynamics of the AFGP, the implications of these results in antifreeze function are also presented.

To prevent the formation of large ice crystals in blood serum and tissue at subzero temperatures, several species, including certain polar fishes and insects have evolved to survive with the help of a special class of antifreeze proteins. These proteins inhibit the growth of ice crystals by lowering the freezing point, with only a small effect on the melting temperature. This noncolligative property manifests as a thermal hysteresis between cooling and warming cycles. There are two major classes of proteins that are responsible for the antifreeze function; proteins that are glycosylated, known as antifreeze glycoproteins, and antifreeze proteins (AFP), which lack glycosylation[6,9]. Extensive structural and dynamic characterization of the AFP's has been done, while such details are limited in the case of AFGPs.

There are eight known fractions of AFGP that range in molecular mass from 33.7 to 2.6 kD [5,10,11], and each consists of a number of repeating units of alanine-alanine-threonine, with minor sequence variations. AFGP8 is the shortest, with 4 repeating units, and AFGP1 the longest, with 50 repeating units. The threonines are glycosylated at the Cβ position with the disaccharide β-D-galactopyranosyl- (1,3) –2-acetamido-2- deoxy-α-D-galactopyranose. [10] In this work, AFGP8s from the Greenland cod, *Boreogadus saida,* in which alanine is substituted for proline at positions 4 and 10 (Figure 1) were studied. NMR methods have been used to extensively study backbone and side-chain dynamics of proteins, but a majority of these have focused on other relaxation related internal motional parameters [12]. Conformation exchange to determine rotational barrier energies has also been carried out in several model protein systems [13], as well as on amino groups of DNA oligomers [14]. However, all these studies have been confined to room temperatures (> 0° C), and to our knowledge this is the first study where the temperature range includes the supercooled state of water as well. Quantum chemical

calculations provide additional understanding at the molecular level and are consistent with results from NMR experiments.

II Materials and Methods

II.1 Chemically labeled antifreeze glycoprotein:

AFGP from the Greenland cod *Boreogadus saida* were prepared as previously described [5,15]. AFGP8 was dimethylated at the N-terminus according the method of described by Means and Feeney [16] and the modified proteins are referred to as m*AFGP8. The efficiency of the methylation was assessed by fluorescamine assay [17]. Figure 1 shows the schematic presentation of the m*AFGP8 with the isotopically enriched N-terminal methyl groups highlighted along with the amino acid sequence. A total of 60 μL protein sample dissolved in D_2O (99.9 % pure, Isotech Inc.,) was taken in a 3mm (o.d., outer diameter) thin walled NMR tube (Wilmad Inc.,).

II.2 Nuclear Magnetic Resonance Spectroscopy:

Solution state ^{13}C-NMR spectra were recorded in D_2O at 14.1 T on a Varian INOVA600. Direct ^{13}C NMR spectra were obtained with ^{1}H broadband decoupling. ^{13}C spin-lattice relaxation times were determined from 256 K to 298 K using a conventional inversion recovery experiment. Spin-lattice relaxation rates ($R_1 = T_1^{-1}$) of the carbons were measured using refocused-INEPT (insensitive nuclei enhanced by polarization transfer) based inversion recovery experiments [18]. The defocusing and refocusing delays of the experiments were 1.7 and 1.1 ms, respectively. A total of 18 recovery delays between 0 to 5 seconds, with duplicate experiments were performed. Effective spin-spin relaxation rates ($R_2^* = 1/T_2^*$) for the carbon resonances are estimated from the full-width at half-maximum from high resolution one-dimensional NMR spectra at each temperature. 64 transients with an equilibrium recovery delay of 10 s were used in the R_1 and R_2^* measurements. During the relaxation recovery period in the R_1 experiments as well as during acquisition in both R_1 and R_2^*, protons are decoupled by the multiple-pulse

sequence WALTZ-16 [19] (field strength 3.5 kHz, centered at 2.8 ppm). Two-dimensional constant time HSQC (CT-HSQC) [20] were performed under the same conditions as those of the relaxation experiments [21]. Probe temperature for the solution-state NMR experiments was calibrated by using the chemical shift difference between the methyl and hydroxyl group in neat methanol [22]. The cooling rate between the temperatures was approximately 0.1° C/minute and more than 15 minutes were allowed for temperature stabilization between the experiments. Chemical shifts of the carbons were referenced at 25 °C with respect to $CDCl_3$ in the outer tube (center of the triplet at 77.0 ppm). Solid-state ^{13}C NMR data were obtained as described in detail previously [8].

II.3 Analysis of the ^{13}C relaxation data:

Dynamics of the N-terminal dimethyl group were analyzed by treating the two ^{13}C nuclei as an isolated homonuclear two-spin system (^{13}C-^{13}C) undergoing chemical exchange. This approximation can be justified by the fact that the dynamics of the carbons is governed predominantly by the restricted rotation about the N-CA bond and the relaxation contributions (dipolar and chemical shift anisotropy of the methyl group). Cross correlation between the dipolar and CSA, mechanisms are averaged out due to protein decoupling [23]. The master equation governing the expectation values of the polarization operators ($\langle S_z \rangle$) of the two carbons

(labeled L and R) can then written as [24,25],

$$\frac{d}{dt}\begin{pmatrix}\langle S_z^L(t)\rangle \\ \langle S_z^R(t)\rangle\end{pmatrix} = -\begin{pmatrix}(R_1^L + k_r) & (k_r - \sigma_{LR}) \\ (k_r - \sigma_{RL}) & (R_1^R + k_r)\end{pmatrix}\begin{pmatrix}\langle S_z^L(t)\rangle - S_0^L \\ \langle S_z^R(t)\rangle - S_0^R\end{pmatrix} \quad (1)$$

where, R_1^L, R_1^R are the self-relaxation rates of carbons L and R respectively, σ_{LR} the cross-relaxation rate, k_r is the rate of rotation of the dimethyl groups around the N-CA bond and S_o is the equilibrium population. The general solutions for Eq.[1] are

$$\langle S_z^L(t)\rangle = C_1 \exp(\lambda_1 t) + C_2 \exp(\lambda_2 t) \quad (2a)$$

$$\langle S_z^R(t)\rangle = D_1 \exp(\lambda_1 t) + D_2 \exp(\lambda_2 t) \quad (2b)$$

$$\text{where } \lambda_{1,2} = -\Sigma \pm \Delta, \quad (3)$$

$$\text{with } \Sigma = (R_1^L + R_1^S)/2 + k_r \quad (4a)$$

$$\Delta = (\delta^2 + (k_r - \sigma_{LR})^2)^{1/2} \quad (4b)$$

$$\delta = (R_1^L - R_1^S)/2 \quad (4c)$$

$$C_{1,2} = (-(\Delta \pm \delta)\, S_0^L \pm (k_r - \sigma_{LR})\, S_0^R)/2\Delta \quad (5a)$$

and

$$D_{1,2} = (\pm (k_r - \sigma_{LR})\, S_0^L + (\Delta \pm \delta)\, S_0^R)/2\Delta \quad (5b)$$

The solutions (Eq.2) can be simplified by noting that the relaxation is dominated by heteronuclear dipolar interactions with the methyl group and the relaxation of the two methyl carbons should be similar ($R_1^L \approx R_1^R = R_1$) and hence $\delta \approx 0$. (Eq. 4c). Thus, the eigenvalues (Eq. 3 and 4) becomes

$$\lambda_1 = -R_1 - \sigma_{LR}; \text{ and } \lambda_2 = -R_1 - 2k_r + \sigma_{LR} \quad (6a,b)$$

The difference in the relaxation rates is due to the effect of rotation and any cross relaxation between the two carbons. Equation 6 can be further simplified as the contributions of σ_{LR} can be safely ignored since the distance between the carbons is 2.5 Å ($\sigma_{LR} \approx$ zero). This approximation is probably not valid if the two nuclei are protons (^1H) instead of ^{13}C, as the dipolar interaction will still be a dominant interaction for relaxation, due to inherently higher values of

gyromagnetic ratio. Thus the difference in the rate of decay of the two carbons is exclusively due to the hindered rotation and Eq.[4-5] can be written as

$\Sigma = R_1 + k_r$; and $\Delta = k_r$ (7a,c)

$C_{1,2} = (-S_0^L \pm S_0^R)/2$ (8a)

$D_{1,2} = (\pm S_0^L - S_0^R)/2$ (8b)

where,

$S_o^+ \equiv S_0^L + S_0^R$; and $S_o^- \equiv S_0^L - S_0^R$ (9a,b),

Representing the sum and difference of the equilibrium distribution of populations between the two states, the general solutions in Eq.[2] can be written in a compact form as

$\langle S_z^L(t)\rangle = S_o^+ \exp(-R_1 t) + S_o^- \exp(-R_1 - 2k_r)$ (10a)

$\langle S_z^R(t)\rangle = S_o^+ \exp(-R_1 t) - S_o^- \exp(-R_1 - 2k_r)$ (10b)

It is straightforward to estimate the rate of rotation by using a non-linear least squared-fitting algorithm to fit the inversion recovery curves to Eq. [10]. As seen by Eq.[10], relaxation of the methyl group is directly modulated by the internal rotation. In the limit that the rotation rate is much slower than the spin-lattice relaxation rate ($k_r \ll R_1$), the recovery non-equilibrium state is mono-exponential by the rate-constant, R_1.

II. 4 Quantum Chemical Calculations:

The potential energy barrier for N,N-dimethyl-alanyl-amide was calculated by varying the C1-N-CA-C dihedral angle in 15° increments. This dihedral angle was fixed during the calculations and all other degrees of freedom were optimized using the program Gaussian98 [26]. The geometries and energies were calculated at the B3LYP/6-31+G(d) level of theory. The three lowest energy structures (at dihedral angles 60°, -75°, and –150°) on the rotational barrier were further optimized without constraints. To ensure these three structures were minima, harmonic

frequency calculations were performed. Additionally, the transition state for inversion of the amine nitrogen was calculated and characterized by a single imaginary frequency.

III Results

III.1 Solution NMR Spectroscopy:

Figure 2a shows examples of proton decoupled one-dimensional ^{13}C-NMR spectra as a function of temperature. Figure 2b shows representative plots from a CT-HSQC experiment performed at supercooled (-17 °C) and room temperature (24 °C) of the m*AFGP8. The temperature range in the supercooled regime is also indicated. The two carbon signals assigned arbitrarily as L and R (for left and right) resonates at 44.40 ppm and 40.97 ppm, respectively. Other naturally abundant carbon signals from the m*AFGP8 are not observed due to low sensitivity. With the current sample conditions, the lowest supercooled temperature of m*AFGP8 attained was –19°C. The intensity of the signals from 'L' carbon increases slowly as the temperature cooled down while the corresponding intensity of the 'R' carbon decreases by the same amount. This suggests that there is a slow inter-conversion between the two conformations, and that at any given temperature the total integrated intensity of the methyl carbons does not change (data not shown). In the solution state temperature range, the chemical shifts of the carbon resonances remain unchanged. On the contrary, the proton resonance from both 'L' and 'R' methyl groups overlap each other in the supercooled state, while at room temperature the 'L' resonance downfield shifted by 0.05 ppm (30 Hz). Figure 3 shows the plots of the effective linewidth (R_2*) of the carbon resonances (full width at half-maximum) as a function of temperature. The error bars in Fig.3 correspond to the digital resolution of the time-domain data, before Fourier transformation (0.4 Hz/pt), and the respective values are listed in table 1. The linewidth of the 'R' carbon in the room temperature (3.1 Hz) almost triples (9.0 Hz) at the supercooled temperature. The corresponding changes observed in the 'L' carbon are much

lower owing to the fact that the relative intensity is also smaller. The spectral changes are completely reproducible under various cooling/heating cycles. Figure 4 shows a representative example from the inversion recovery experiment at the supercooled state (-17 °C, Fig 4a) andat room temperature (+24 °C, Fig 4b). The data clearly show a significantly different time constant of recovery to equilibrium between the two carbons. At all measured temperatures, carbon 'L' recovers much more slowly than 'R'. Figure 4c shows plots of the results of a non-linear least square fit to the experimental data for the 'R' carbon at room temperature (filled circles, continuous lines, T=24 °C) and in the supercooled state (filled squares, dashed lines, T= -17 °C). Figure 5 shows the plot of the temperature dependence of R_1 (spin-lattice relaxation time) estimated from the experimental data for the 'L' and 'R' carbons, along with the nonlinear least-square fit to Eq.[10]. Table 2 lists the estimated values of R_1. Overall relaxation behavior of the carbons are still dictated by the rotational correlation of the m*AFGP8. However, the rates for individual carbons (L and R) differ significantly from each other. 'L' has a much longer decay constant than 'R', but the relative variation as a function of temperature is much less, as seen by the slopes in Figure 5. In comparison to the changes in the linewidth temperature dependence (Figure 3), the R_1 values of both carbons (in particular 'L') are much more sensitive to the processes that govern spin-lattice relaxation times. Though the spectral changes over the temperature range studied show specific signatures of hindered rotation, the changes in the R_1 values are not sensitive enough to estimate the exchange rate with higher accuracy. Based on the experimental data, the rotation rate is estimated to be 0.5 – 1.0 Hz, suggesting strongly that $k_{ex} << R_1$.

III.2 Solid state NMR spectroscopy:

Recently we presented a comprehensive study on the dynamics of m*AFGP (AFGP8 and AFGP2-5) in the presence of ice using solid-state NMR and FT-IR experiments [8]. Figure 6

shows the ^{13}C MAS NMR spectra of m*AFGP8 in D_2O as a function of temperature. Spectra were also acquired in the presence of H_2O under similar conditions (data not shown). The first row of the NMR spectra (figure 6a) corresponds to the room temperature spectrum similar to data shown in Figure 2. Further lowering the sample temperature from the supercooled state (T ≈ –16° C, Figure 2) induced nucleation and formation of ice. Solid-state NMR data obtained in the presence of ice shows the complex nature of the conformational states of the N-terminal dimethyl group and introduces significant changes in the NMR spectra (Fig. 6b, c and d). Intensity of the 'L' carbon increases further following the trend seen upon supercooling while that of the 'R' carbon adopts additional conformational states as seen by additional resonances (Figure 6b). Upon further lowering the temperature, the additional conformational states seem to 'freeze out', that corresponded to distinct chemical environments. Broadening of the resonances close to the originally defined 'R' carbon is due to the presence of additional conformational states as well as effect of lowering the temperature. Dynamics of the N-terminal dimethyl group in m*AFGP8 is predominantly between two conformational states in the room temperature and in supercooled states, while it adopts a rather complex dynamics between multiple states in the solid-state (ice).

III.3 Quantum chemical calculations:

In order to assign the orientation of the dimethyl group relative to the protein backbone, we have also performed quantum chemical calculations. Figure 7 shows the rotational barrier for the dimethyl group. Three energy minimums are present along the rotational barrier that corresponds to the 3 staggered conformers for the N-CA bond. A relatively small energy barrier of ~2.3 kcal/mol separates the structures at –75° and –150° and large barriers of 7.2 and 10.9 kcal/mol separate the 60° structure from the structures at –75° and –150°, respectively. The large rotational barrier to 60° is due to having the methyl groups on the nitrogen pass the peptide

(CA-C bond) backbone and reorientation of the amide side chain to accommodate one of the methyl groups. Although there are three energy minima present in the rotational barrier, the small energy barrier between the –75° and –150° structures would allow rapid inter-conversion and conformational averaging. The rotational barrier between the 60° and the other two minima are larger and not easily surmounted at room temperature. Another possible way to reach the 60° structure is by inversion of the amine nitrogen (see Figure 8) from the -150° structure [27]. The energy barrier from the -150° structure and the inversion transition state structure is 6.4 kcal/mol. Inversion and rotation of the dimethyl group from and to the 60° structure are energetically competing processes. The barriers for leaving the 60° minimum are lower, 3.3 and 4.1 kcal/mole by inversion and rotation respectively.

IV Discussion

IV.1 Time scale of the restricted rotation:

NMR is the best way to investigate dynamical processes at the atomic level and with sufficient resolution to sample motions at multiple time scales. Even though the experimental NMR techniques used to study hindered rotations [28] is not new the applications of these methods to a wider variety of systems continue to increase. The exchange process is generally subdivided into three major time scales, slow, intermediate and fast with reference to the chemical shift difference between the observed sites [25]. Based on this definition the conformational dynamics observed for the dimethyl group at the N-terminal of m*AFGP8 is slow. Slow conformational exchange affects principally the z-magnetization of the system and the spin-lattice relaxation time measurements are ideally suited for studying this process [29]. In this study, ^{13}C NMR time scale is favorable [30] to characterize the hindered rotation, while the proton spectra at the same range of temperatures does not show the conformation exchange effect (data not shown).

The dynamics of the dimethyl group in the solution state (water and supercooled water) is slow and predominantly between two chemically distinct environments. The N-terminal dimethyl groups in the solid state (in the presence of ice) however tend to adopt several additional conformational states as the various states get frozen out. Due to inherently slow conformational dynamics of the dimethyl groups in the solution state even at a wide range of temperature, no attempt has been made to determine to activation parameters. Increasing the temperature further may not be highly suitable for the stability of the protein.

IV. 2 Influence of protein structure:

Is there any influence of the protein structure (backbone or sidechain) on the conformational dynamics of the N-terminal methyl groups? Our results strongly suggest that the dynamics of the dimethyl groups is only locally dictated by the properties of the N-CA bond. Presence of the additional methyl group associated with the first N-terminal residue, alanine probably tends to influence the dihedral angles between the N-CA and CA-C bonds. Quantum chemical calculations performed with the other side-chains (e.g. replacing CH_3 group of alanine by H to become glycine) alter the energy landscape (data not shown). Characterization of restricted rotations has often been confined to small model compounds. One such classic example is the NMR and molecular modeling studies in dimethyl formamide (DMF) [31]. In the case of larger biomolecules, internal rotation of the exocyclic amino groups in double helical DNA molecules has drawn considerable attention from experimental as well theoretical studies. In all these cases, the internal rotation is always associated with local geometry of the molecule.

The chemical labeling method used to modify the N-terminal of the AFGP is based on reductive alkylation and has been used to label the lysine sidechains in larger proteins. Jentoft el al., [32] have used ^{13}C NMR spectroscopy of follow the chemical labeling procedure and no indication of conformational exchange of the dimethyl groups were presented. The most likely

reason that they might not have observed these effects at the spectrometer frequency (carbon resonating at 45.284 MHz, T=25° C) is due to lower sensitivity and resolution. At lower resonating frequencies, the difference in the chemical shifts will be smaller than the exchange rate ($|\omega_L - \omega_R| < k_r$, instead of $|\omega_L - \omega_R| \approx k_r$) and moving the exchange mechanism to intermediate time scale, this manifests itself predominantly as a change in the lineshape. More importantly, these experiments were performed only at one temperature and hence it is not surprising that the exchange behavior is missed all together. In summary, our results suggest that neither the backbone nor the sidechain structure of m*AFGP8 influence the N-terminal rotational dynamics.

IV. 3 Mechanisms of exchange

The NMR results indicate that two conformers for the dimethyl groups are predominant. The quantum chemical calculations show that three minimums are present along the rotational barrier. Two of these minimums are separated by a small barrier that is easily surmounted at room temperature and lead to conformational averaging between these structures. The larger barrier separating the 60° structure from the other two minimums can be accessed either by rotation or inversion of the amine nitrogen (see Figure 8). The energy barriers for these two processes are similar and likely compete when the conformation of the dimethyl group changes. These calculations are consistent with the NMR results. At room temperature, there is conformational averaging between the -75° and -150° structures leading to one ^{13}C signal and the structure at 60° is responsible fro the second ^{13}C signal. As the temperature is lowered, the barrier between the -75° and -150° structures becomes more difficult to pass leading to a more complex NMR spectra.

IV. 4 Dynamics in the supercooled state

Characterization of biomolecules dissolved in supercooled water has been implicated only recently as a means to obtain improved structural and dynamic properties of proteins and

nucleic acids and to gain insights into protein hydration and cold denaturation [33]. As AFGP tend to function at supercooled temperatures, structure and dynamics characterization at this state take on particular importance. Recently, Graether et al., [34] have investigated the dynamics of antifreeze protein I (AFP-I) in the supercooled state and found no significant change in the overall rotational motion. Translational dynamic characterization of AFGP molecules in the supercooled states has also been investigated recently by our group [35]. Site-selective chemical labeling method presented here will be useful to monitor the overall rotational motion of AFGP molecules.

V Conclusions

The discovery of antifreeze glycoproteins 30 years ago has opened an exciting field of research into the role of these proteins in inhibiting the growth of ice at subzero temperatures. Despite the significant amount of work, and extensive reviews representing many disciplines, from ice physics to molecular biology and physiology, little is known about the structure and dynamics of these proteins in the presence of ice. The lack of information is mainly due to difficulties of the existing experimental methods in obtaining details at the molecular level. Furthermore, few methods are sensitive enough to measure consistent and reliable parameters at low temperatures. Additional difficulties in determining the three-dimensional structures of AFGP arise from the presence of glycosylated sugar residues and the absence of high-level expression systems. Chemical labeling with rare isotopes is a viable alternative to obtain structural and dynamical information using modern NMR methods. This approach greatly increases the sensitivity of the ^{13}C signals and allows us to obtain specific motional information. The site-directed methylation of the AFGP N-terminus is very important for this investigation because any other method for chemical modification, for example altering the hydroxyl groups

of the side chain sugar residues, may interfere with the antifreeze activity of the protein [36] and modification of the N-terminus of the protein by methylation has been shown to have no effect on the antifreeze activity [37].

Although good quality NMR data are obtained when the N-terminal alanine of AFGP is modified to ^{13}C-labeled N,N-dimethylalanine, and the methyl groups tends to undergo conformation exchange. In order to make sure that this dynamics does not affect AFGP conformations, a complete characterization of the restricted rotation was performed. NMR experiments as a function of temperature from the solution state (water) to the solid state (ice) including the supercooled state show: (a) The N-terminal dimethyl group interchanges between two unequally populated conformational states at room temperature as well as supercooled temperatures; (b) In the solid-state (ice), additional conformational states were observed due to freezing out of the various intermediate geometries; (c) Quantum chemical calculations on our chosen model compound support the NMR characterization; and (d) The effect of protein structure on the rotational dynamics is limited to the choice of the first N-terminal residue. In summary, this modification does not affect either the backbone or side chain conformation of the protein, thus allowing us to attribute the observed change in the dynamics of the methyl groups to that of AFGP.

Acknowledgements

The authors thank the other members of AFGP research group (D. Nguyen, S. Zepeda, Professors Y. Duan and Q.Z. Li) for many discussions. Thanks to S.P. Mielke for critical reading of the manuscript and many suggestions. Solid-state NMR data (Figure 6) was kindly provided by Dr. B.L. Phillips. NT was supported in part by NIH grants (HL57810-01 & HL61204). This work was performed under the auspices of the U.S. Department of Energy by the University of California, Lawrence Livermore National Laboratory under Contract No. W-7405-Eng-48 (VVK).

Figure Captions

Figure 1: Schematic diagram of the N-terminal modified AFGP8 (m*AFGP8). Each of the Three amino-acid repeats (AAT or PAT), with the threonines (shown by larger letters) glycosylated at the Cβ positions with the disaccharide. The two-^{13}C labeled methyl groups and the rotation of the di-methyl group is also pointed out. Atom names used for describing the N,N-dimethylalanine are shown.

Figure 2: Solution state NMR data. (a) One-dimensional ^{13}C-NMR (^{1}H-decoupled) spectra of m*AFGP8 as a function of temperature through the supercooled state. "L" and "R" arbitrarily refer to the two carbons. (b) Constant time HSQC (CT-HSQC) spectra of m*AFGP8 in the supercooled and room temperature.

Figure 3: Plot of the effective line width (half-width at half-maximum) of the "L" and "R" carbons in m*AFGP8, shown by circles and squares respectively. The error bars are obtained from the digital resolution of the time domain-data. Vertical dashed-line is drawn at 0° C.

Figure 4: NMR spectra of m*AFGP8 as a function of the post-inversion recovery delay in the T_1 measurements at room temperature (a) and in the supercooled temperature (b). The plot of the recovery curves used to measure the T_1 values is shown in (c). The error bars are obtained from duplicate measurements.

Figure 5: Plot of the experimental spin-lattice relaxation rate constants (R_1) as a function of temperature for the "L" (circles) and "R" (squares) carbons of m*AFGP8. R_1 values were obtained as described in the materials and methods.

Figure 6: CP-MAS ^{13}C-NMR spectra of m*AFGP8 as function of temperature in D_2O. Spectrum (a) is acquired in the solution state, while spectra (b) through (f) are in the solid-state.

Figure 7: Rotation barrier along the N-CA dihedral angle of N,N-dimethyl alanyl amide with the related minimum energy structures.

Figure 8: Minimum and transition state structures long the N-CA dihedral angle of N,N-dimethyl alanyl amide. Each structure is oriented to look towards the N-CA bond with the sidechain methyl and alpha hydrogen at the same position. The values by the arrows are the energy barriers (kcal/mole) separating the structures except to the transition. The values to the transition state are the energy difference between the depicted structures.

Tables

Table 1: R_2^* values of N-terminal dimethyl carbons.

T (C)	Effective Line Width (R_2^*)	
	Carbon R	Carbon L
23.53	3.14	3.10
20.87	3.15	3.03
18.21	3.21	3.03
15.55	3.31	2.97
12.90	3.42	2.99
10.24	3.56	3.03
7.58	3.72	2.97
5.00	3.87	2.86
3.59	4.03	2.84
2.26	4.17	2.89
0.93	4.32	2.88
-0.40	4.57	2.83
-1.73	4.57	2.84
-3.06	4.75	2.83
-4.39	5.04	2.83
-5.71	5.08	3.01
-7.04	5.38	2.81
-8.37	5.85	2.83
-9.70	6.17	2.83
-11.03	6.55	2.85
-12.36	6.88	2.93
-13.69	7.77	2.91
-15.02	7.82	2.92
-16.35	8.53	2.99
-17.68	9.07	2.97

Table 2: R_1 values of N-terminal dimethyl carbons.

T (C)	Spin Lattice Relaxation time (R_1)	
	Carbon R	Carbon L
24.46	1.23 ± 0.09	0.26 ± 0.11
19.54	1.40 ± 0.08	0.37 ± 0.15
15.55	1.42 ± 0.17	0.29 ± 0.02
11.57	1.53 ± 0.52	0.16 ± 0.02
7.58	1.70 ± 0.17	0.10 ± 0.03
3.59	1.74 ± 0.12	0.17 ± 0.04
-0.40	1.80 ± 0.13	0.13 ± 0.11
-4.39	1.90 ±0.34	0.19 ± 0.04
-8.37	1.91 ± 0.07	0.15 ± 0.05
-11.03	2.02 ± 0.13	0.19 ± 0.04
-13.69	2.10 ± 0.18	0.12 ± 0.07
-16.35	2.32 ± 0.43	0.47 ± 0.28
-19.01	2.35 ± 0.68	0.74 ± 0.58

References

[1] D. Suckau, M. Mak, and M. Przybylski, Proceedings of the National Academy of Sciences of the United States of America **89** (12), 5630 (1992); K. M. Fazili, M. M. Mir, and M. A. Qasim, Biochemistry and Molecular Biology International **31** (5), 807 (1993); C. M. Tann, D. F. Qi, and M. D. Distefano, Current Opinion in Chemical Biology **5** (6), 696 (2001).

[2] A. Bax and S. Grzesiek, Accounts of Chemical Research **26** (4), 131 (1993); G. Wagner, Nature Structural Biology **4** (SUPPS), 841 (1997); A. E. Ferentz and G. Wagner, Quarterly Reviews of Biophysics **33** (1), 29 (2000).

[3] T. Yamazaki, T. Otomo, N. Oda, Y. Kyogoku, K. Uegaki, N. Ito, Y. Ishino, and H. Nakamura, Journal of the American Chemical Society **120** (22), 5591 (1998); N. K. Goto and L. E. Kay, Current Opinion in Structural Biology **10** (5), 585 (2000); J. Kikuchi, T. Asakura, K. Hasuda, T. Ito, K. Ohwaku, H. Araki, and M. P. Williamson, Journal of Biochemical and Biophysical Methods **42** (1-2), 35 (2000).

[4] R. L. Giuntoli, L. I. Stoykova, D. R. B. Glllies, and M. C. Glick, European Journal of Biochemistry **225** (1), 159 (1994); J. R. Huth, C. A. Bewley, B. M. Jackson, A. G. Hinnebusch, G. M. Clore, and A. M. Gronenborn, Protein Science **6** (11), 2359 (1997).

[5] R. E. Feeney and Y. Yeh, Adv Protein Chem **32**, 191 (1978).

[6] Y. Yeh and R. E. Feeney, Chemical Reviews **96** (2), 601 (1996).

[7] P. L. Davies and B. D. Sykes, Current Opinion in Structural Biology **7** (6), 828 (1997); M. M. Harding, P. I. Anderberg, and A. D. J. Haymet, European Journal of Biochemistry **270** (7), 1381 (2003).

[8] N. M. Tsvetkova, B. L. Phillips, V. V. Krishnan, R. E. Feeney, W. H. Fink, J. H. Crowe, S. H. Risbud, F. Tablin, and Y. Yeh, Biophysical Journal **82** (1), 464 (2002).

[9] M. M. Harding, L. G. Ward, and A. D. J. Haymet, European Journal of Biochemistry **264** (3), 653 (1999); S. P. Graether and B. D. Sykes, European Journal of Biochemistry **271** (16), 3285 (2004).

[10] R. E. Feeney, T. S. Burcham, and Y. Yeh, Annu Rev Biophys Biophys Chem **15**, 59 (1986).

[11] A. L. De Vries, Methods Enzymol **127**, 293 (1986).

[12] A. G. Palmer, Annual Review of Biophysics and Biomolecular Structure **30**, 129 (2001).

[13] C. L. Perrin, Accounts of Chemical Research **22** (8), 268 (1989).

[14] L. D. Williams, N. G. Williams, and B. R. Shaw, Journal of the American Chemical Society **112** (2), 829 (1990); J. G. Moe and I. M. Russu, Nucleic Acids Research **18** (4), 821 (1990); R. Michalczyk and I. M. Russu, Biophysical Journal **76** (5), 2679 (1999).

[15] D. T. Osuga and R. E. Feeney, J Biol Chem **253** (15), 5338 (1978).

[16] G. E. Means and R. E. Feeney, Analytical Biochemistry **224** (1), 1 (1995); G. E. Means and R. E. Feeney, Journal of Food Biochemistry **22** (5), 399 (1998).

[17] S. Undenfriend, S. Stein, P. Bohlen, and W. Dairman, Science **178**, 871 (1972).

[18] G. Morris, A. and R. Freeman, Journal of the American Chemical Society **101** (3), 760 (1979).

[19] A. Shaka, J., J. Keeler, and R. Freeman, Journal of Magnetic Resonance **53** (2), 313 (1983).

[20] G. W. Vuister and A. Bax, Journal of Magnetic Resonance **98** (2), 428 (1992).

[21] D. States, J., R. Haberkorn, A., and D. Ruben, J., Journal of Magnetic Resonance **48** (2), 286 (1982).

[22] A. L. Van Geet, Analytical Chemistry **42**, 679 (1970); D. S. Raiford, C. L. Fisk, and E. D. Becker, Analytical Chemistry **51**, 2050 (1979).

[23] J. Boyd, U. Hommel, and I. D. Campbell, Chemical Physics Letters **175** (5), 477 (1990).

[24] J. H. Noggle and R. E. Schirmer, *The nuclear Overhauser effect; chemical applications*. (Academic Press, New York,, 1971).

[25] J. Sandström, *Dynamic NMR spectroscopy*. (Academic Press, London ; New York, 1982).

[26] M. J. Frisch, G. W. T., H. B. Schlegel, G. E. Scuseria, M. A. Robb, J. R. Cheeseman, V. G. Zakrzewski, J. A. Montgomery, Jr., R. E. Stratmann, J. C. Burant, S. Dapprich, J. M. Millam, A. D. Daniels, K. N. Kudin, M. C. Strain, O. Farkas, J. Tomasi, V. Barone, M. Cossi, R. Cammi, B. Mennucci, C. Pomelli, C. Adamo, S. Clifford, J. Ochterski, G. A. Petersson, P. Y. Ayala, Q. Cui, K. Morokuma, D. K. Malick, A. D. Rabuck, K. Raghavachari, J. B. Foresman, J. Cioslowski, J. V. Ortiz, A. G. Baboul, B. B. Stefanov, G. Liu, A. Liashenko, P. Piskorz, I. Komaromi, R. Gomperts, R. L. Martin, D. J. Fox, T. Keith, M. A. Al-Laham, C. Y. Peng, A. Nanayakkara, C. Gonzalez, M. Challacombe, P. M. W. Gill, B. Johnson, W. Chen, M. W. Wong, J. L. Andres, C. Gonzalez, M. Head-Gordon, E. S. Replogle, and J. A. Pople., Gaussian 98 (Gaussian Inc.,, Pittsburgh PA, 1998).

[27] C. Kieft, European Journal of Organic Chemistry (19), 3279 (2000).

[28] H. S. Gutowsky and C. H. Holm, Journal of Chemical Physics **25**, 1228 (1956).

[29] A. D. Bain and J. A. Cramer, Journal of Physical Chemistry **97** (12), 2884 (1993); A. D. Bain, Biochemistry and Cell Biology-Biochimie Et Biologie Cellulaire **76** (2-3), 171 (1998).

[30] D. Stephenson, S. and G. Binsch, Journal of Magnetic Resonance **32** (1), 145 (1978).

[31] J. B. Lambert and J. W. Keepers, Journal of Magnetic Resonance **38**, 233 (1980); R. Konrat and H. Sterk, Journal of Physical Chemistry **94** (4), 1291 (1990).

[32] N. Jentoft and D. G. Dearborn, J Biol Chem **254** (11), 4359 (1979); J. E. Jentoft, N. Jentoft, T. A. Gerken, and D. G. Dearborn, J Biol Chem **254** (11), 4366 (1979).

[33] L. Poppe and H. Vanhalbeek, Nature Structural Biology **1** (4), 215 (1994); J. J. Skalicky, D. K. Sukumaran, J. L. Mills, and T. Szyperski, Journal of the American Chemical Society **122** (13), 3230 (2000); J. J. Skalicky, J. L. Mills, S. Sharma, and T. Szyperski, Journal of the American Chemical Society **123** (3), 388 (2001).

[34] S. P. Graether, C. M. Slupsky, P. L. Davies, and B. D. Sykes, Biophysical Journal **81** (3), 1677 (2001).

[35] V. V. Krishnan, W. H. Fink, R. E. Feeney, and Y. Yeh, Biophysical Chemistry **110** (3), 223 (2004).

[36] S. K. Komatsu, A. L. DeVeries, and R. E. Feeney, Journal of Biological Chemistry **245**, 2909 (1970).

[37] K. F. Geoghegan, D. T. Osuga, A. I. Ahmed, Y. Yeh, and R. E. Feeney, Journal of Biological Chemistry **255**, 663 (1980).

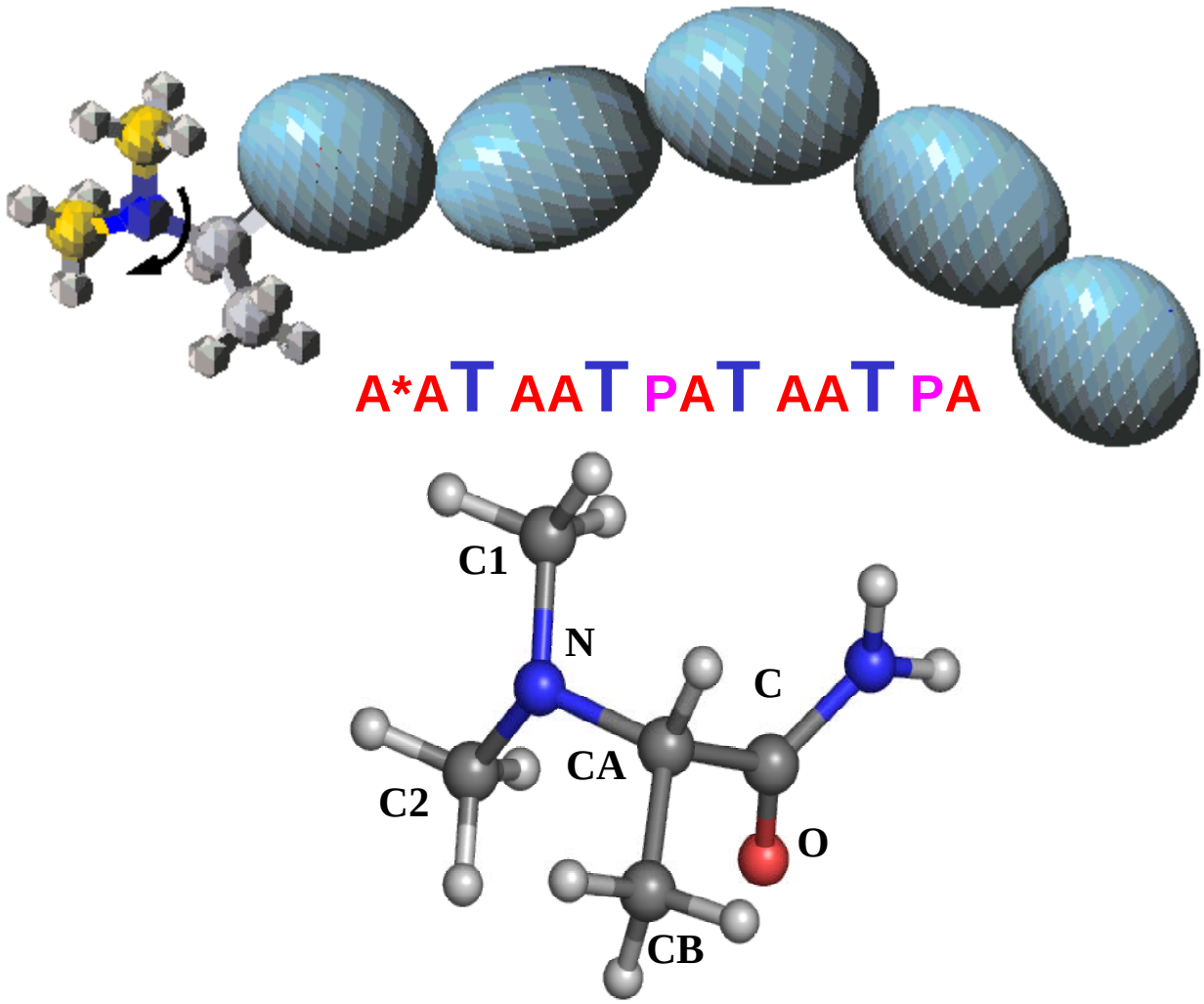

Figure 1

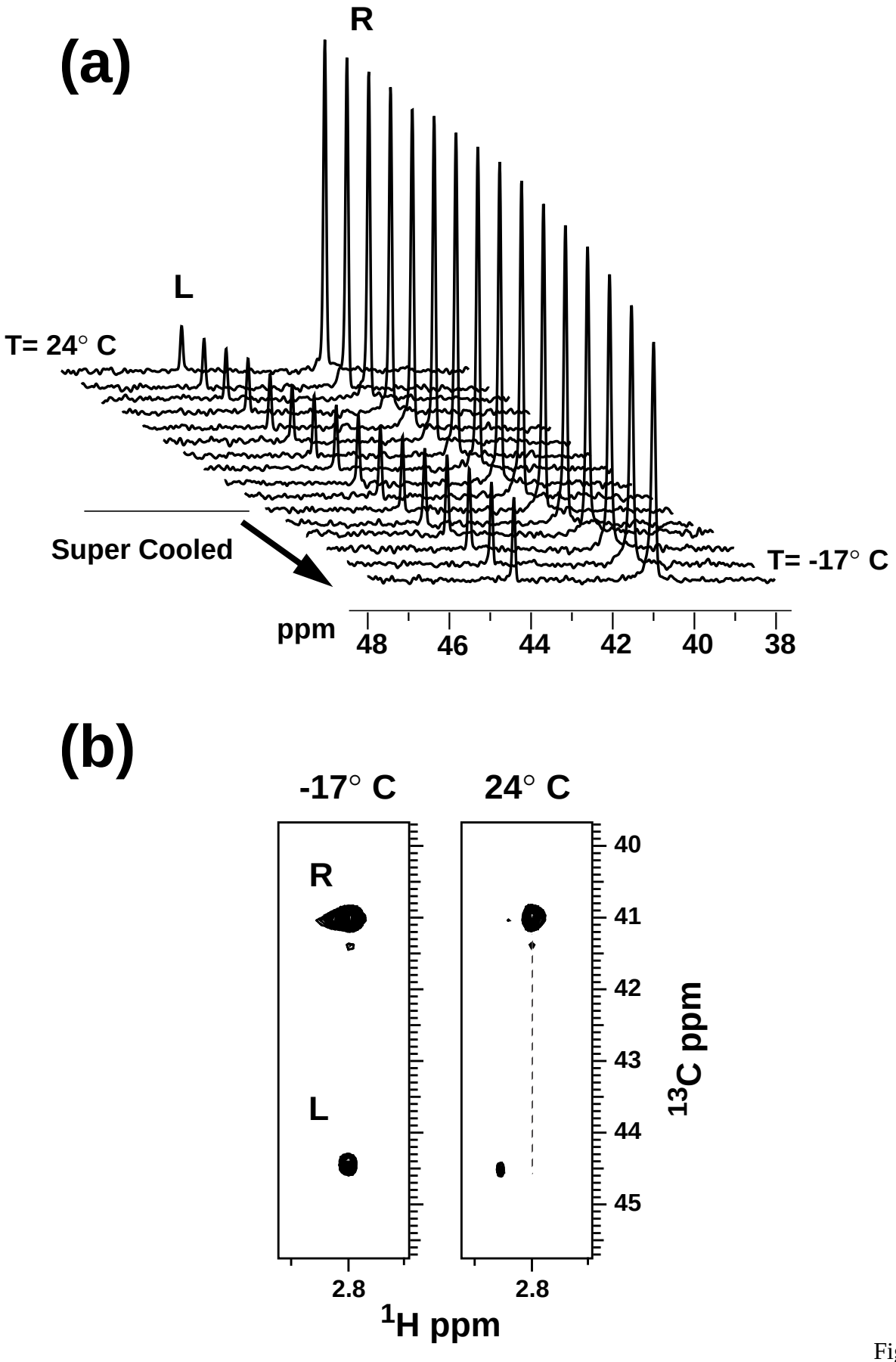
(a)
R
L
T= 24° C
Super Cooled
T= -17° C
ppm
48
46
44
42
40
38
(b)
-17° C
24° C
R
L
40
41
42
43
44
45
13C ppm
2.8
2.8
1H ppm

Figure 2

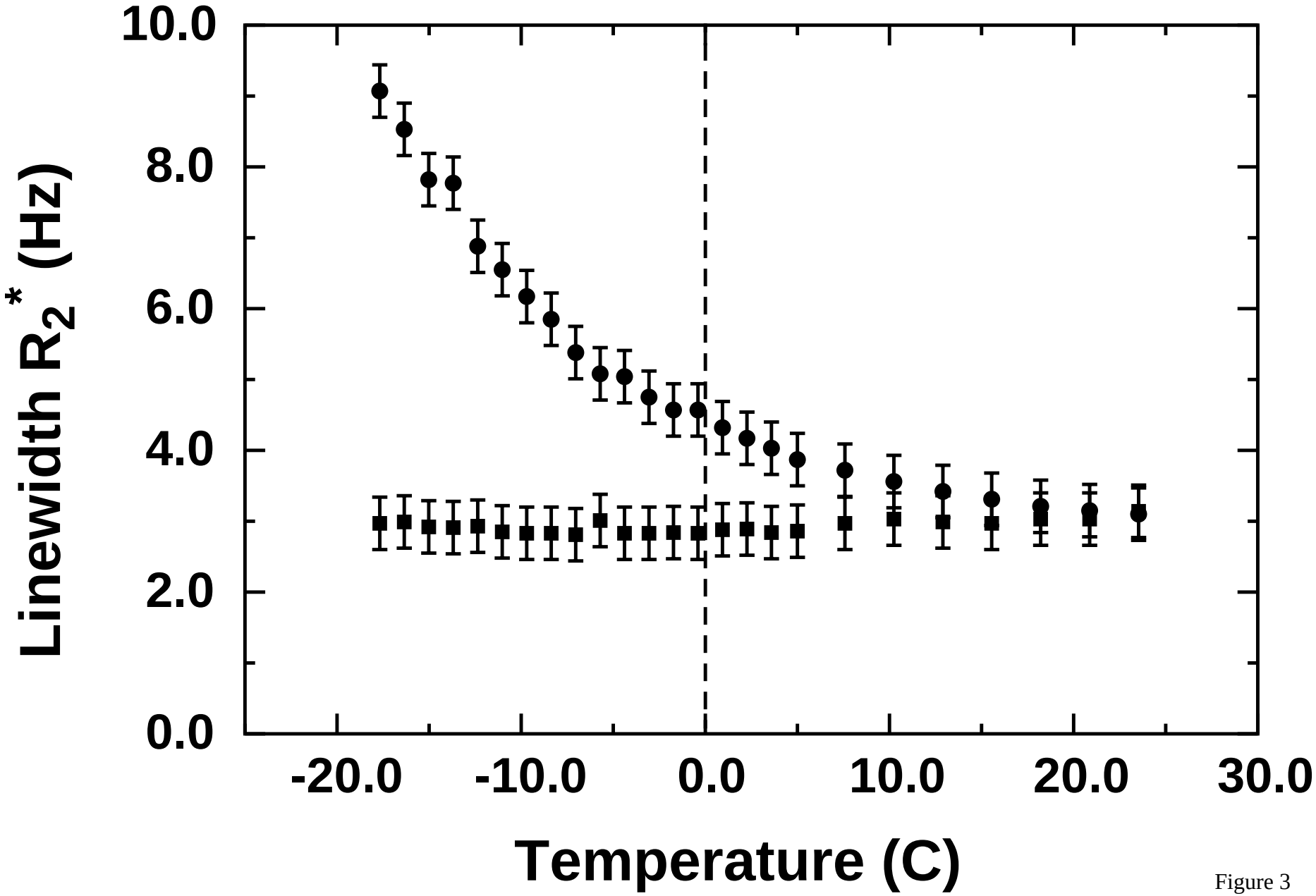
10.0
8.0
6.0
4.0
2.0
0.0
Linewidth R_2^* (Hz)
-20.0
-10.0
0.0
10.0
20.0
30.0
Temperature (C)

Figure 3

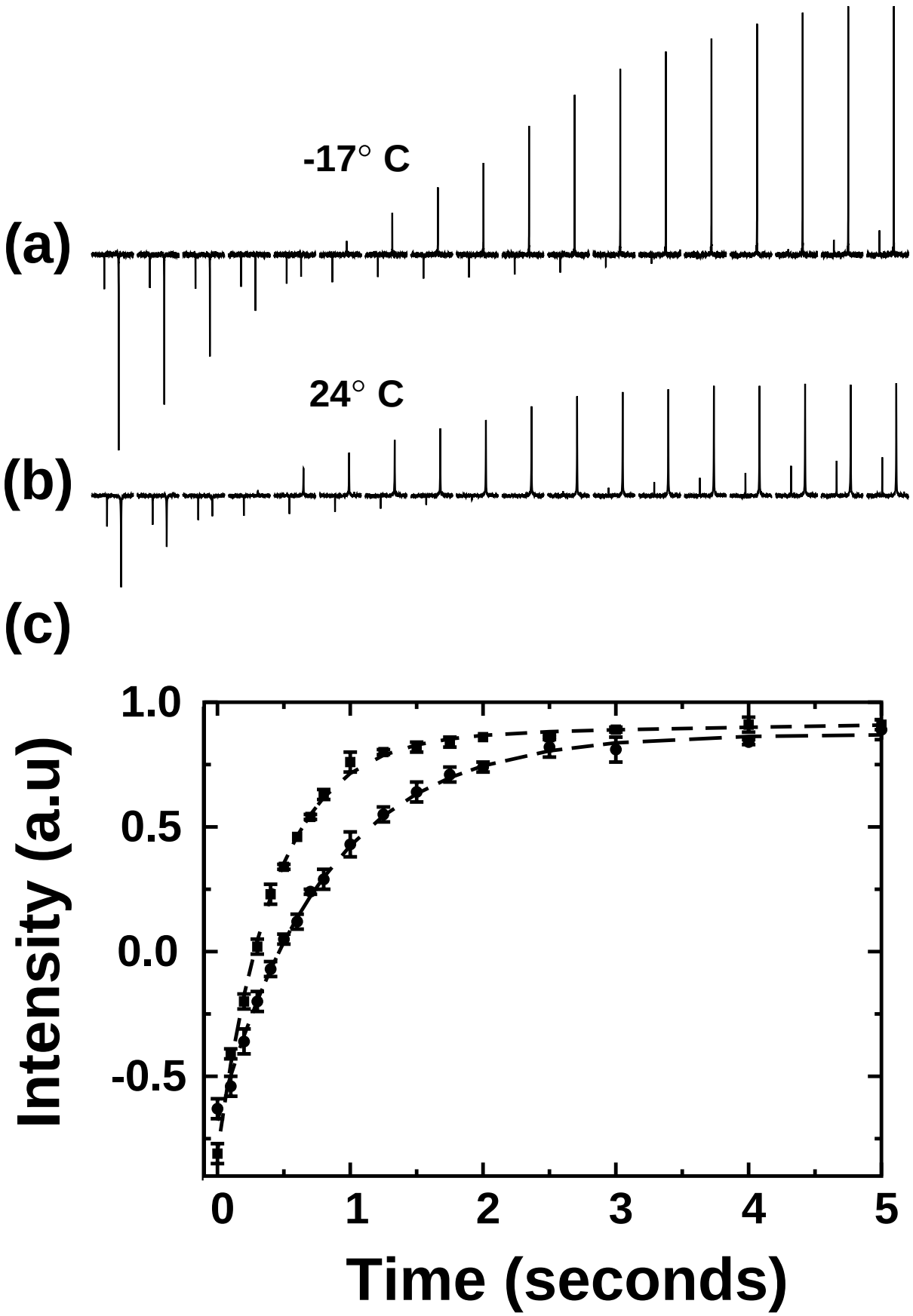

Figure 4

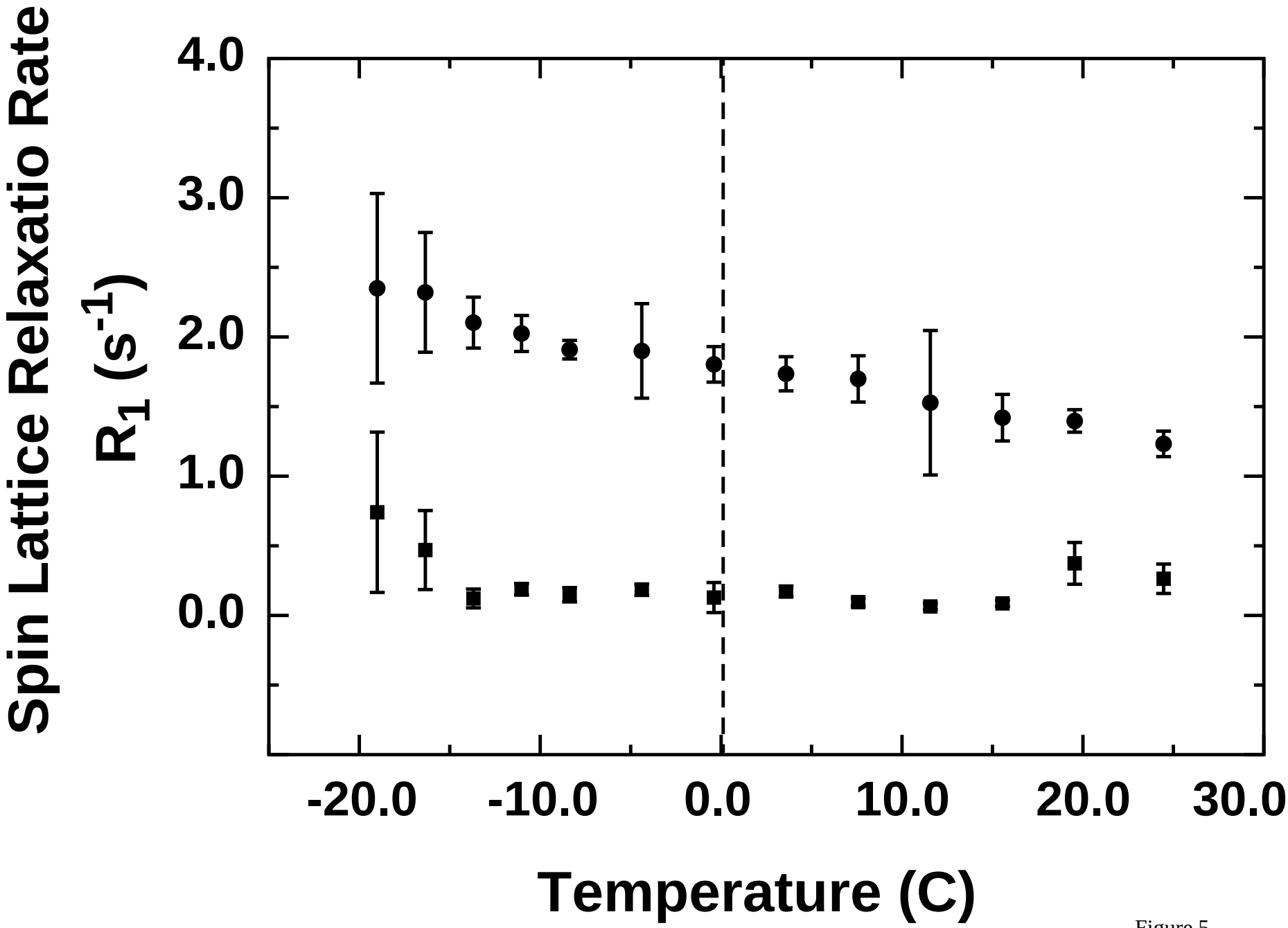
Spin Lattice Relaxatio Rate
R_1 (s^{-1})
4.0
3.0
2.0
1.0
0.0
-20.0
-10.0
0.0
10.0
20.0
30.0
Temperature (C)

Figure 5

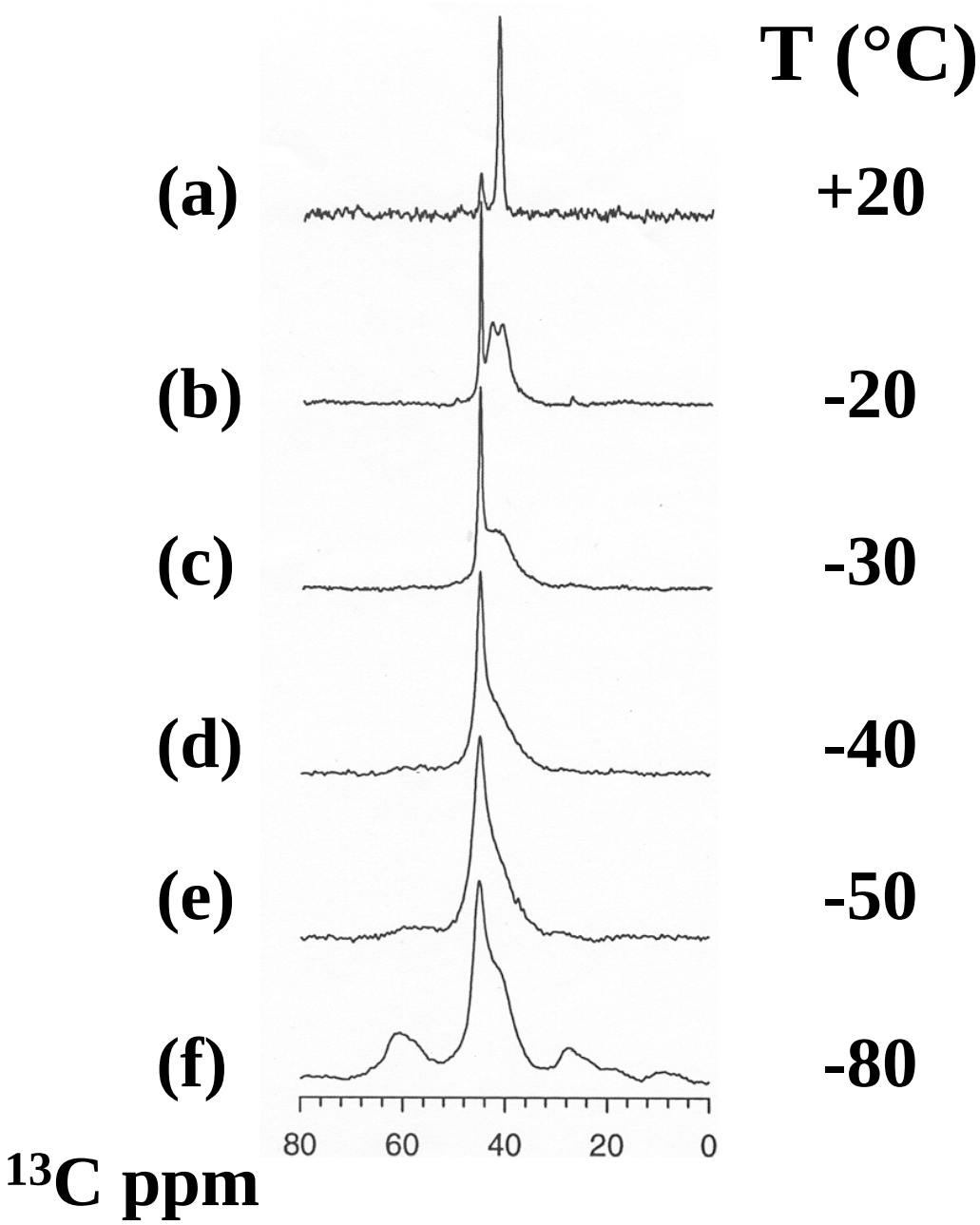

Figure 6

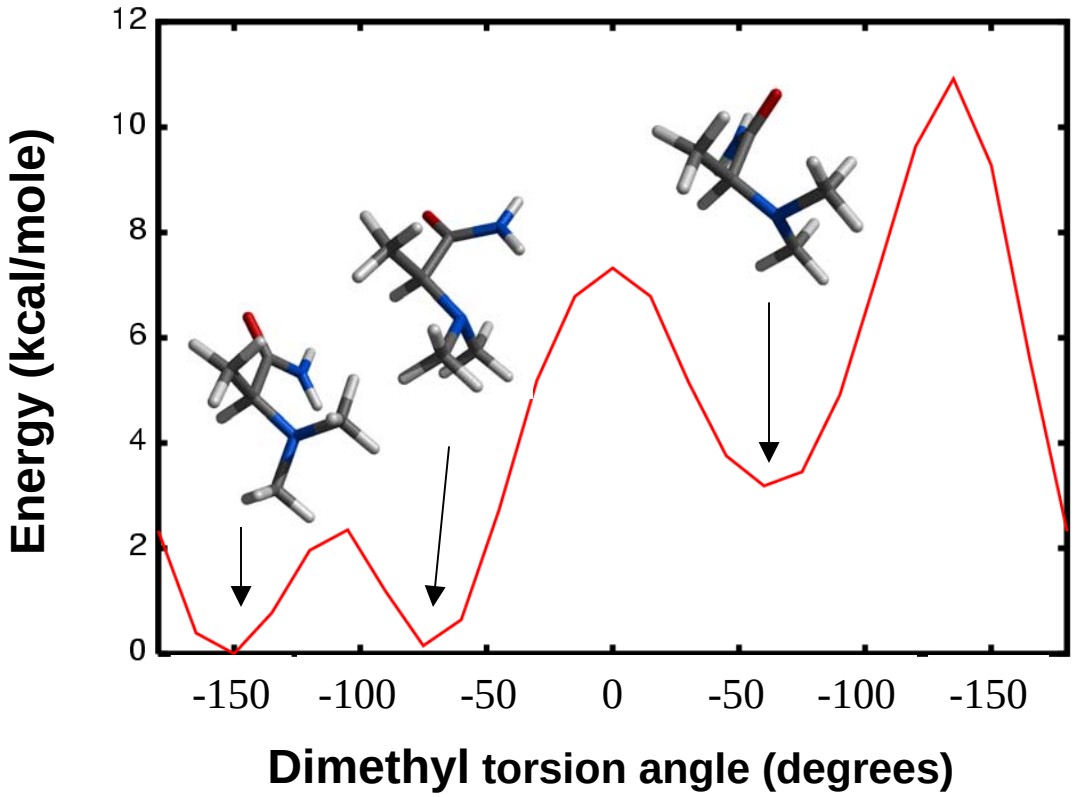
Energy (kcal/mole)
12
10
8
6
4
2
0
-150
-100
-50
0
-50
-100
-150
Dimethyl torsion angle (degrees)

Figure 7

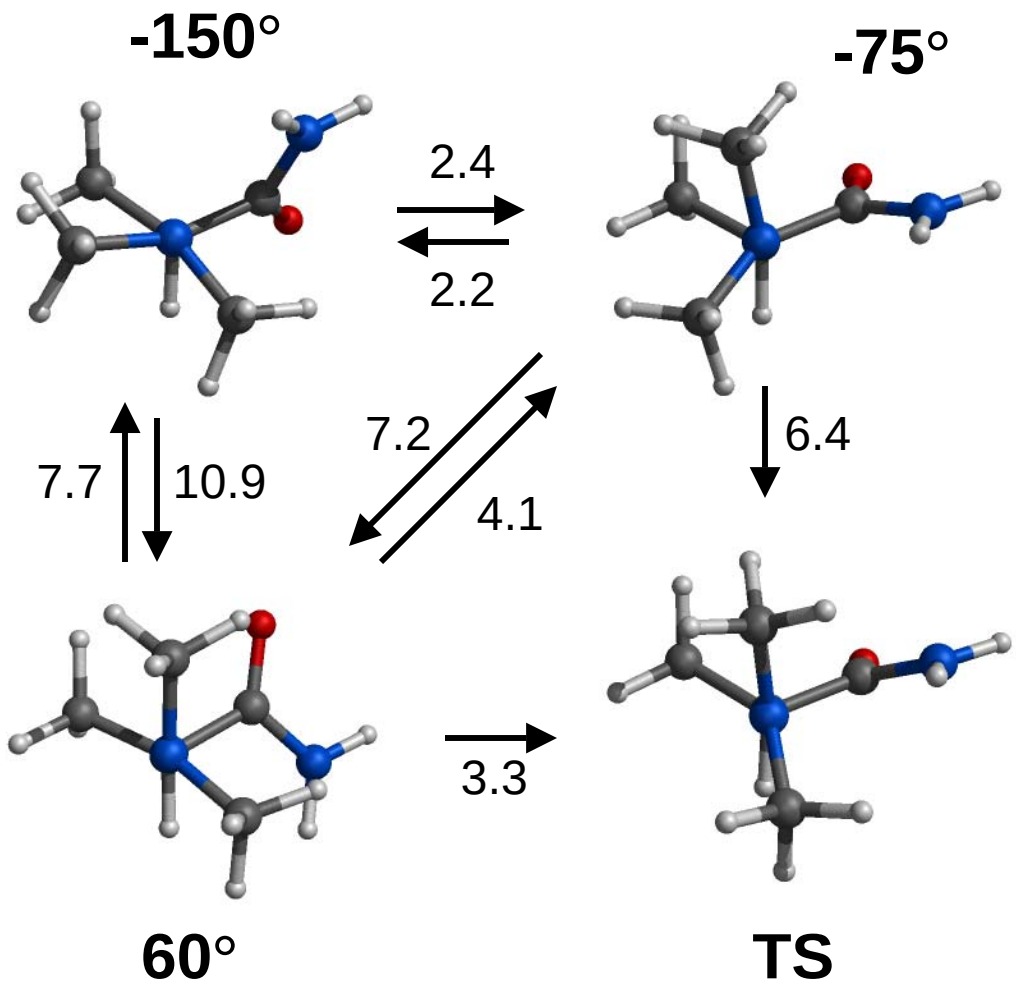

Figure 8